数理解析研究所講究録
1135巻 2000年 52-76

Travelling Front Solutions Arising in a Chemotaxis–Growth Model

広島商船高等専門学校 舟木 弥夫(MitsuoFunaki)
広島大学数理分子生命科学研究科 三村 昌泰(MasayasuMimura)
宮崎大学工学部 辻川 亨(TohruTsujikawa)

Abstract. We consider a bistable reaction-diffusion-advection system describing the growth of biological individuals which move by diffusion and chemotaxis. In order to know the dynamics of growth patterns arising in this system, we use the singular limit analysis to study the transversal stability of travelling front solutions in a strip domain. It is shown that travelling front solutions are transversally stable when the chemotactic effect is weak and, when it becomes stronger, they are destabilized. Moreover, numerical simulations demonstrate that the destabilized solution evolves into complex patterns with dynamic network–like structures.

1 Introduction

Some biological individuals have a tendency to move preferentially toward higher concentrations of chemicals in their environment, which is called *chemotaxis*. It is experimentally observed, for instance, that bacteria called *E.coli*, which move by not only diffusion but also chemotaxis and grow by performing cell–division, to exhibit complex spatio–temporal colony patterns (Budrene and Berg [3, 4]).

For theoretical understanding of such chemotactic growth patterns, several continuum as well as discrete models have been proposed so far (see Woodward et al. [23], Stevens [18], Ezoe et al. [5], Kawasaki and Shigesada [11], for instance). In the previous paper (Mimura and Tsujikawa [13]), we considered a chemotaxis–growth model to investigate the influence of the chemotactic effect on growth patterns under the situation where nutrients are constantly supplied. For the density of biological individuals $u(t,\mathbf{x})$ and the concentration of a chemical attractant $v(t,\mathbf{x})$ at time t and position $\mathbf{x}$ in the plane $\mathbf{R}^2$, the model is described by

$$\begin{cases} \dfrac{\partial u}{\partial t} = d_u\Delta u - \nabla(u\nabla\chi(v)) + f(u) \\ \qquad\qquad\qquad\qquad t>0,\ \mathbf{x}\in\mathbf{R}^2, \\ \dfrac{\partial v}{\partial t} = d_v\Delta v + \alpha u - \beta v \end{cases} \tag{1.1}$$

where the migration of individuals consists of two effects, "randomly walking" by diffusion and "directed movements" by chemotaxis. d_u and d_v are the diffusion rates of u and

v, respectively. $\chi(v)$ is the chemotactic sensitivity function of the chemical attractant, satisfying $\chi'(v) > 0$ for $v > 0$, in a sense that the flux rate of individuals is the response to its chemical gradient distributed in space. Several plausible forms of $\chi(v)$ are proposed (Ford and Lauffenburger [8]). A simple example is $\chi(v) = kv$ with a constant $k > 0$. The growth term $f(u)$ takes the form $f(u) = (g(u) - \delta)u$ with growth rate $g(u)$ and degradation rate δ modelling to the stress due to waste products (see [20], for instance). If $g(u)$ includes the Allee effect (see [15], for instance), the functional form of $g(u)$ is threshold–like. For suitable δ, we may assume $f(u)$ to take cubic-like nonlinearity, that is, $f(u)$ satisfies $f(0) = f(u_*) = f(u^*) = 0$ with two constants u_* and u^* $(0 < u_* < u^*)$ where $f'(0) < 0$ and $f'(u^*) < 0$. For the chemical attractant α is the production rate and β the degradation rate, which are both positive constants.

For the system (1.1) we consider the situation where (i) the chemical attractant diffuses much faster than the movement of individuals; (ii) individuals mainly move by chemotaxis rather than diffusion. In order to model this situation, we conveniently introduce a small parameter $\varepsilon > 0$ to rewrite (1.1) in the following form:

$$\begin{cases} \dfrac{\partial u}{\partial t} = \varepsilon^2 \Delta u - \varepsilon \nabla(u \nabla \chi(v)) + f(u) \\ \qquad\qquad\qquad\qquad\qquad\qquad t > 0,\ \mathbf{x} \in \mathbf{R}^2, \\ \dfrac{\partial v}{\partial t} = \Delta v + u - \gamma v \end{cases} \tag{1.2}$$

where γ is a positive constant and $f(u)$ has three zeros $0, a$ and 1 ($0 < a < 1$). Hereafter, we simply specify $f(u)$ as $f(u) = u(1-u)(u-a)$ with $0 < a < 1$. It is noted that (1.2) has three spatially constant equilibria $(u, v) = (0, 0)$, $(a, a/\gamma)$ and $(1, 1/\gamma)$ for which $(0, 0)$ and $(1, 1/\gamma)$ are both stable, while $(a, a/\gamma)$ is unstable, that is, (1.2) is a bistable system. For the boundary condition to (1.2), it is biologically natural to impose

$$\lim_{|\mathbf{x}| \to \infty} (u, v)(t, \mathbf{x}) = (0, 0) \qquad t > 0. \tag{1.3}$$

If there is no chemotactic effect in the system, (1.2) with (1.3) simply reduces to the following scalar bistable reaction-diffusion equation

$$\frac{\partial u}{\partial t} = \varepsilon^2 \Delta u + f(u) \qquad t > 0,\ \mathbf{x} \in \mathbf{R}^2 \tag{1.4}$$

with the boundary condition

$$\lim_{|\mathbf{x}| \to \infty} u(t, \mathbf{x}) = 0 \qquad t > 0. \tag{1.5}$$

The qualitative behavior of solutions of (1.4), (1.5) has been intensely investigated by many authors (see Aronson and Weinberger [1, 2], for instance). Suppose that the initial

data $u(0,\mathbf{x})$ is given such that the region where $u(0,\mathbf{x}) > a$ is bounded and relatively large. Then, the behaviour of solutions to (1.4) essentially consists of two stages: (i) There occur internal layers which separate $\mathbf{R}^2$ into two qualitatively different regions where u nearly takes the value either 1 or 0, and (ii) if $\int_0^1 f(u)du > 0$ (resp. < 0), the region where $u(t,\mathbf{x})$ is nearly 1 (we may call it the aggregating region) expands (resp. shrinks) uniformly (Jones [9, 10]). If ε is sufficiently small, the behavior of internal layers is more precisely analyzed by using the singular limit analysis ([14]). Taking the limit $\varepsilon \downarrow 0$, the layers become interfaces, say $\Gamma(t)$, which are the boundary between two regions $\Omega_1(t) = \{\mathbf{x} \in \mathbf{R}^2 | u(t,\mathbf{x}) = 1\}$ and $\Omega_0(t) = \{\mathbf{x} \in \mathbf{R}^2 | u(t,\mathbf{x}) = 0\}$, and the time evolution of $\Gamma(t)$ is approximately described by

$$V(t) = \varepsilon(c - \varepsilon\kappa(t)), \tag{1.6}$$

where $V(t)$ is the normal velocity at $\Gamma(t)$, which is oriented from $\Omega_1(t)$ to $\Omega_0(t)$ and $\kappa(t)$ is the curvature at $\Gamma(t)$. c is the velocity of the travelling front solution $u(x-ct)$ of the 1–dimensional problem

$$\begin{cases} u_t = u_{xx} + f(u) & t > 0,\ x \in \mathbf{R} \\ u(t,-\infty) = 1 \text{ and } & u(t,\infty) = 0. \end{cases}$$

If $\int_0^1 f(u)du > 0$ (resp. < 0), we know $c > 0$ (resp. < 0) (see Fife and McLeod [7], for example). In particular, if the shape of $\Gamma(0)$ is given by a ball with radius r_0, $\Gamma(t)$ is also a ball with radius $r(t)$, satisfying the simple differential equation

$$\dot{r} = \varepsilon(c - \frac{\varepsilon}{r}) \qquad t > 0 \tag{1.7}$$

with $r(0) = r_0$. Thus, in the absence of chemotaxis, the pattern dynamics is simply that u expands uniformly and its shape becomes asymptotically disk–like.

In this paper, we assume $\int_0^1 f(u)du > 0$ or $0 < a < 1/2$ to consider the situation where the aggregating region uniformly expands in the absence of a chemotactic effect, and study how this effect influences the pattern expansion. More precisely speaking, since several forms of the sensitive function $\chi(v)$ are proposed, as we already noted, it is our purpose to understand the dependence on the functional form of $\chi(v)$ to the stability of the expanding pattern. Let us first show some numerical computations of (1.2), (1.3). To do it, we introduce a parameter $k > 0$ so that $\chi(v) = k\chi_0(v)$ with $\max_{v>0} \chi_0'(v) = 1$, so that k measures the intensity of the chemotactic effect. For computations, we specify $\chi_0(v)$ as $\chi_0(v) = 8v^2/3(3+v^2)$ (see Schaaf [17], for instance). The first case is restricted to the radially symmetric situation with $|\mathbf{x}| = r$, that is, the initial condition is given by $u(0,r) = 1$ for $0 < r < r_0$ and $u(0,r) = 0$ for $r_0 < r$ with some constant r_0 and $v(0,r) \equiv 0$ for any $r > 0$. Because of radial symmetry, the solution of (1.2), (1.3) is represented as

$(u,v)(t,r)$ where there occurs an internal layer in $u(t,r)$, whose location is described by a circle in such a way that u takes nearly 1 inside and nearly 0 outside of the circle. When k is small, it is obviously expected that the circle of internal layer uniformly expands with asymptotically constant velocity. We note that the velocity is slightly slower than in the case $k=0$. When k increases, the influence of chemotaxis on the expanding circle becomes apparent by establishing a disk–like equilibrium solution. When k is large, there is no more disk–like equilibrium solution, the initial circle shrinks and finally becomes extinct ([13]). These phenomena suggest that the chemotactic effect induces a suppression of expanding patterns.

Next we numerically consider the stability of these radially symmetric patterns. Let the initial shape of $u(0,x)$ be slightly deformed from the circle. When k is small, the deformation instantly decays and the shape of pattern recovers to be circular. However, when k increases, the situation is changed. The initial circular shape is destabilized so that there appears a flower–like pattern. When k increases further, the circular shape is destabilized to be a star–like one with multi–branches and then the resulting pattern exhibits tip–splitting and coalescing phenomena, so that dynamic network–like structure is observed (Figure 1a). When k further increases, the instability of the circular shape happends as similar as the initiation in Figure 1a and then each branch proceeds as if it were a 2–dimensional travelling finger wave (Figure 1b). These numerical results indicate that the chemotactic effect provides not only suppression of expanding of patterns but also shape–destabilization of patterns.

In order to analytically understand the dependency of the chemotactic effect on these properties, we consider the transversal stability of 1–dimensional travelling front solutions $(u,v)(x-\theta t,y)$ with velocity θ of (1.2) in the strip domain $\Omega_\ell=\{(x,y)\in\mathbf{R}^2|\,-\infty<x<\infty, 0<y<\ell\}$ with width $\ell>0$, where the boundary conditions are

$$\begin{cases} (u,v)(t,-\infty,y)=(1,\dfrac{1}{\gamma}) & t>0,\ 0<y<\ell \\ (u,v)(t,+\infty,y)=(0,0) & t>0,\ 0<y<\ell, \end{cases} \tag{1.8}$$

and

$$\begin{cases} (\dfrac{\partial u}{\partial y},\dfrac{\partial v}{\partial y})(t,x,0)=(0,0) & t>0,\ -\infty<x<+\infty \\ (\dfrac{\partial u}{\partial y},\dfrac{\partial v}{\partial y})(t,x,\ell)=(0,0) & t>0,\ -\infty<x<+\infty. \end{cases} \tag{1.9}$$

This paper is organized as follows: In Section 2, we apply the singular perturbation method to (1.2) with a sufficiently small $\varepsilon>0$ and show the existence of 1–dimensional travelling front solutions $(U^\varepsilon,V^\varepsilon)(z)$ ($z=x-\varepsilon\theta(\varepsilon)t$). We note that $V^\varepsilon(z)$ is smooth

and $U^\varepsilon(z)$ possesses a single internal layer, which becomes an interface as $\varepsilon \downarrow 0$. The dependency of k on the velocity $\theta(\varepsilon)$ is shown in Figure 2. We will show that there is $k^*(\varepsilon)$ with $\lim_{\varepsilon \downarrow 0} k^*(\varepsilon) = k^* = 2\sqrt{\gamma}c/\chi_0'(\frac{1}{2\gamma})$ such that $\theta(\varepsilon) > 0$ for $0 < k < k^*(\varepsilon)$, while $\theta(\varepsilon) < 0$ for $k^*(\varepsilon) < k$ in Proposition 1 (ii). Consequently, one finds that chemotaxis plays the role of suppression of expanding patterns.

In Section 3, we use the singular limit analysis as $\varepsilon \downarrow 0$ and study the transversal stability of the travelling front solutions $(U^\varepsilon, V^\varepsilon)(z)$ in the strip domain Ω_ℓ. In order to show it, we study the distribution of eigenvalues of the linearized eigenvalue problem of (1.2), (1.8), (1.9) around the planar travelling front solution, depending on the parameters k and ℓ. Our result (Theorem 2) reveals that the transversal stability crucially depends on the sign of $\chi_0''(v_{\rm I})$ where $v_{\rm I}$ is the value of the 1–dimensional travelling front solution $V^\varepsilon(z)$ on the interfacial point obtained by taking the limit $\varepsilon \downarrow 0$. If $\chi_0''(v_{\rm I}) \leq 0$, the solution is stable for any $k > 0$ and $\ell > 0$. However, if $\chi_0''(v_{\rm I}) > 0$, the stability depends on values of k. When k is small, travelling front solutions are always stable for any fixed $\ell > 0$, while they are destabilized when k increases. It should be noted that when they are destabilized, the fastest growing mode m of the perturbations given in the interface is $O(\varepsilon^{-\frac{1}{3}})$ for sufficiently small $\varepsilon > 0$, that is, the fastest growing wavelength $2\ell/m$ is $O(\varepsilon^{\frac{1}{3}})$. This indicates that the destabilized pattern does not initially depend on the width ℓ but on the smallness of ε. We remark that this behavior is observed also in usual activator–inhibitor reaction–diffusion systems [19]. In Section 4, we give some remarks on our results.

2 Travelling front solutions

We will briefly demonstrate how 1–dimensional travelling front solutions of (1.2), (1.8) can be constructed, by using the well known singular perturbation methods. To do it, we introduce the travelling coordinate $z = x - \varepsilon\theta t$ with velocity $\varepsilon\theta$ in (1.2). It turns out that the travelling front solution $(u, v)(z)$ satisfies the following system:

$$\begin{cases} 0 = \varepsilon^2 u_{zz} + \varepsilon\theta u_z - \varepsilon k \left[u\chi_0'(v)v_z\right]_z + f(u) \\ \\ 0 = v_{zz} + \varepsilon\theta v_z + u - \gamma v \end{cases} \qquad z \in \mathbf{R} \tag{2.1}$$

with the boundary conditions

$$(u, v)(-\infty) = (1, \frac{1}{\gamma}) \text{ and } (u, v)(+\infty) = (0, 0). \tag{2.2}$$

We first construct the outer and inner approximate solutions of (2.1) with (2.2), taking the limit $\varepsilon \downarrow 0$.

2.1 Outer and inner solutions

By putting $\varepsilon = 0$ in (2.1), the lowest outer solution (u^0, v^0) of (2.1) satisfies

$$\begin{cases} 0 = f(u) \\ \\ 0 = v_{zz} + u - \gamma v \end{cases} \qquad z \in \mathbf{R}. \tag{2.3}$$

From the first equation of (2.3) with the boundary conditions (2.2), we may take $u^0(z)$ as

$$u^0(z) = \begin{cases} 0 & (z > 0) \\ \\ 1 & (z < 0). \end{cases} \tag{2.4}$$

Substituting it into the second equation of (2.3), we obtain $v^0(z)$ as

$$v^0(z) = \begin{cases} \dfrac{1}{2\gamma} \exp(-\sqrt{\gamma} z) & (z > 0) \\ \\ \dfrac{1}{\gamma} - \dfrac{1}{2\gamma} \exp(\sqrt{\gamma} z) & (z < 0), \end{cases} \tag{2.5}$$

which belongs to $C^1(\mathbf{R})$. $(u^0, v^0)(z)$ is called an *outer* solution of (2.1), (2.2) in $\mathbf{R}$. Since $u^0(z)$ is discontinuous at $z = 0$, it is not a good approximate solution of (2.1) in a neighborhood of $z = 0$, so that we have to look for another approximate solution there.

In order to construct an approximate solution in a neighborhood of $z = 0$, we introduce the usual streched variable $\xi = z/\varepsilon$ and rewrite (2.1) as

$$\begin{cases} 0 = \tilde{u}_{\xi\xi} + \{\theta - k\chi_0'(\tilde{v})\tilde{v}_z\}\tilde{u}_\xi - \varepsilon k\{\chi_0'(\tilde{v})\tilde{v}_z\}_z\tilde{u} + f(\tilde{u}) \\ \\ 0 = \tilde{v}_{\xi\xi} + \varepsilon^2\{\theta\tilde{v}_\xi + \tilde{u} - \gamma\tilde{v}\} \end{cases} \qquad \xi \in \mathbf{R}, \tag{2.6}$$

where $(\tilde{u}, \tilde{v})(\xi) = (u, v)(\varepsilon\xi)$. Putting $\varepsilon = 0$ in (2.6) and noting $v^0(0) = 1/2\gamma$, we obtain

$$\begin{cases} 0 = \tilde{u}_{\xi\xi} + \{\theta - k\chi_0'(\tilde{v})\tilde{v}_z\}\tilde{u}_\xi + f(\tilde{u}) \\ \\ 0 = \tilde{v}_{\xi\xi} \end{cases} \qquad \xi \in \mathbf{R} \tag{2.7}$$

with the boundary conditions

$$\begin{cases} \tilde{u}(-\infty) = 1, \qquad \tilde{u}(+\infty) = 0 \\ \\ \tilde{v}(\pm\infty) = \dfrac{1}{2\gamma}. \end{cases} \tag{2.8}$$

Since the second equation of (2.7) with (2.8) leads $\tilde{v}(\xi) \equiv 1/2\gamma$, the first equation of (2.7) is

$$0 = \tilde{u}_{\xi\xi} + \{\theta + \frac{k}{2\sqrt{\gamma}}\chi_0'(\frac{1}{2\gamma})\}\tilde{u}_\xi + f(\tilde{u}). \tag{2.9}$$

In order to solve the equation (2.9) with (2.8), we need the following lemma:

LEMMA 1 (Fife and McLeod [7]). *For any fixed* $\zeta \in (0,1)$, *there uniquely exists* c *such that the following problem has a unique monotone decreasing solution* $W(\xi;c)$:

$$\begin{cases} 0 = W_{\xi\xi} + cW_\xi + f(W) & \xi \in \mathbf{R} \\ W(-\infty) = 1, W(+\infty) = 0, & W(0) = \zeta. \end{cases} \tag{2.10}$$

Furthermore, if $\int_0^1 f(u)du > 0$ (*resp.* < 0), *then* $c > 0$ (*resp.* < 0).

Lemma 1 indicates that a solution $\tilde{u}$ of (2.9) with (2.8) is given by $\tilde{u}(\xi) = W(\xi)$ with $\theta^*(k) = c - k\chi_0'(1/2\gamma)/2\sqrt{\gamma}$. $(\tilde{u},\tilde{v})(z/\varepsilon)$ is called an *inner* solution in a neighborhood of $z = 0$.

2.2 Existence of 1–dimensional travelling front solutions

By matching the outer and inner solutions obtained above, travelling front solutions of the problem (2.1), (2.2) can be constructed (see Fife [6], Mimura et al. [12], for example). The result is stated as follows:

THEOREM 1. *Fix* $k > 0$ *arbitrarily. There is* $\varepsilon_0 > 0$ *such that for any* $\varepsilon \in (0,\varepsilon_0)$ (2.1), (2.2) *has a solution* $(U^\varepsilon, V^\varepsilon)(z)$ *with* $\theta = \theta(\varepsilon;k)$ *satisfying*

$$\lim_{\varepsilon\downarrow 0}\theta(\varepsilon;k) = \theta^*(k) = c - \frac{k}{2\sqrt{\gamma}}\chi_0'(\frac{1}{2\gamma}). \tag{2.11}$$

The solution $(U^\varepsilon, V^\varepsilon)$ *is represented as*

$$U^\varepsilon(z) = W(z/\varepsilon) + p^\varepsilon(z) \quad \textit{and} \quad V^\varepsilon(z) = v^0(z) + q^\varepsilon(z),$$

where $(p^\varepsilon, q^\varepsilon)$ *becomes an error term with respect to small* $\varepsilon > 0$ *by the following convergences;*

$$\begin{cases} \lim_{\varepsilon\downarrow 0} U^\varepsilon(z) = u^0(z) & \textit{uniformly in} \quad (-\infty,-\delta)\cup(\delta,+\infty) \\ \lim_{\varepsilon\downarrow 0} V^\varepsilon(z) = v^0(z) & \textit{uniformly in} \quad \mathbf{R} \end{cases} \tag{2.12}$$

with any small constant $\delta > 0$ *and*

$$\begin{cases} \lim_{\varepsilon \downarrow 0} \tilde{u}^{\varepsilon}(\xi) = W(\xi) & \text{in } C^2_{c.u.}(\mathbf{R})\text{-sense} \\ \lim_{\varepsilon \downarrow 0} \tilde{v}^{\varepsilon}(\xi) = \dfrac{1}{2\gamma} & \text{in } C^2_{c.u.}(\mathbf{R})\text{-sense,} \end{cases} \tag{2.13}$$

where $(\tilde{u}^{\varepsilon}, \tilde{v}^{\varepsilon})(\xi) = (U^{\varepsilon}, V^{\varepsilon})(\varepsilon\xi)$.

By (2.11), we immediately obtain

PROPOSITION 1. (i) *When* $\int_0^1 f(u)du \leq 0$ ($c \leq 0$), $\theta^*(k) < 0$ *always holds for any* $k > 0$. (ii) *When* $\int_0^1 f(u)du > 0$ ($c > 0$), *there is the critical value* $k^* = 2\sqrt{\gamma}c/\chi_0'(\frac{1}{2\gamma})$ *such that* $\theta^*(k) > 0$ *for any* $0 < k < k^*$, *while* $\theta^*(k) < 0$ *for any* $k > k^*$.

For the case (ii) of Proposition 1, the dependency of $\theta^*(k)$ and $\theta(\varepsilon; k)$ on k is shown in Figure 2. The uniquness of travelling front solution of (2.1), (2.2) is numerically confirmed, although it has been still unsolved. Since $\varepsilon c = \varepsilon\theta(\varepsilon; 0)$ is the velocity of the travelling front solution of (2.1), (2.2) in the absence of chemotaxis ($k = 0$), (2.11) indicates that chemotaxis suppresses the expansion of patterns.

3 Transversal stability of travelling front solutions

In Section 1, by numerical simulations, we found that chemotaxis effects destabilization of patterns. For this purpose, we study the transversal stability of travelling front solutions $(U^{\varepsilon}, V^{\varepsilon})(z)$ in a strip domain Ω_{ℓ}. We first define the *linealized* stability of travelling front solutions of (1.2), (1.8), (1.9) as follows:

DEFINITION. A travelling front solution of (1.2), (1.8), (1.9) is *transversally stable* except for translational invariance in x, if and only if zero is a simple eigenvalue of the eigenvalue problem associated with the linealized system of (1.2), (1.8), (1.9) around the travelling front solution and the remaining spectrum is contained in a closed sector lying in the left half of the complex plane (see Volpert et al. [22], for instance). The travelling front solution is *unstable* if it is not stable.

We only study the distribution of eigenvalues of the eigenvalue problem of the linearized system of (1.2), (1.8), (1.9) around the travelling front solutions $(\hat{u}^{\varepsilon}, \hat{v}^{\varepsilon})(z, y) = (U^{\varepsilon}, V^{\varepsilon})(z)$ with velocity $\varepsilon\theta(\varepsilon; k)$ in the strip domain $\Omega_{\ell} = \mathbf{R} \times (0, \ell)$. Here we write $\theta(\varepsilon; k)$ as $\theta(\varepsilon)$

for simplicity. The eigenvalue problem for $(p,q)(z,y)$ associated with (1.2), (1.8), (1.9) is given by

$$\begin{cases} \lambda p = & [\varepsilon^2(\dfrac{\partial^2}{\partial z^2}+\dfrac{\partial^2}{\partial y^2})+\varepsilon\theta(\varepsilon)\dfrac{\partial}{\partial z}-\varepsilon k\{(\chi_0'(\hat{v}^\varepsilon)\hat{v}_z^\varepsilon)\dfrac{\partial}{\partial z} \\ & +(\chi_0'(\hat{v}^\varepsilon)\hat{v}_z^\varepsilon)_z\}+f'(\hat{u}^\varepsilon)]p-\varepsilon k[\hat{u}^\varepsilon\chi_0'(\hat{v}^\varepsilon)(\dfrac{\partial^2}{\partial z^2}+\dfrac{\partial^2}{\partial y^2}) \\ & +\{\hat{u}^\varepsilon\chi_0''(\hat{v}^\varepsilon)\hat{v}_z^\varepsilon+(\hat{u}^\varepsilon\chi_0'(\hat{v}^\varepsilon))_z\}\dfrac{\partial}{\partial z}+(\hat{u}^\varepsilon\chi_0''(\hat{v}^\varepsilon)\hat{v}_z^\varepsilon)_z]q \\ \lambda q = & \ p+\{(\dfrac{\partial^2}{\partial z^2}+\dfrac{\partial^2}{\partial y^2})+\varepsilon\theta(\varepsilon)\dfrac{\partial}{\partial z}-\gamma\}q \end{cases} \tag{3.1}$$

with the boundary conditions

$$\begin{cases} p(\pm\infty,y)=0, \quad q(\pm\infty,y)=0, \quad 0<y<\ell \\ \dfrac{\partial p}{\partial y}(z,0)=0, \quad \dfrac{\partial q}{\partial y}(z,0)=0, \quad z\in\mathbf{R} \\ \dfrac{\partial p}{\partial y}(z,\ell)=0, \quad \dfrac{\partial q}{\partial y}(z,\ell)=0, \quad z\in\mathbf{R}. \end{cases}$$

For $(p,q)(z,y)\in L^2(\Omega_\ell)\times L^2(\Omega_\ell)$, we define $(p_m,q_m)(z)$ ($z\in\mathbf{R}$, $m=0,1,2,\cdots$) by

$$p_m(z)=\int_0^\ell p(z,y)Y_m(y)dy, \qquad q_m(z)=\int_0^\ell q(z,y)Y_m(y)dy,$$

where

$$Y_m(y)=\begin{cases} \dfrac{1}{\sqrt{\ell}} & \text{for } m=0 \\ \sqrt{\dfrac{2}{\ell}}\cos(\dfrac{m\pi y}{\ell}) & \text{for } m\geq 1. \end{cases}$$

Then $(p,q)(z,y)$ is expanded as

$$p(z,y)=\sum_{m=0}^{\infty}p_m(z)Y_m(y), \qquad q(z,y)=\sum_{m=0}^{\infty}q_m(z)Y_m(y)$$

in $L^2(\Omega_\ell)$. It thus follows from (3.1) that the equations for $(p_m,q_m)(z)$ with $\omega=m\pi/\ell$ are given by

$$\begin{cases} \lambda p_m=(L^\varepsilon-\varepsilon^2\omega^2)p_m-N^{\varepsilon,\omega}q_m \\ \lambda q_m=p_m+(M^\varepsilon-\omega^2)q_m \\ p_m,q_m\in C^2_{unif}(\mathbf{R}), \end{cases} \qquad z\in\mathbf{R} \tag{3.2}$$

where

$$L^\varepsilon \equiv \varepsilon^2 \frac{d^2}{dz^2} + \varepsilon\{\theta(\varepsilon) - k\chi_0'(V^\varepsilon)V_z^\varepsilon\}\frac{d}{dz} - \varepsilon k\{\chi_0'(V^\varepsilon)V_z^\varepsilon\}_z + f'(U^\varepsilon),$$

$$N^{\varepsilon,\omega} \equiv \varepsilon k[U^\varepsilon\chi_0'(V^\varepsilon)\{\frac{d^2}{dz^2} - \omega^2\} + \{U_z^\varepsilon\chi_0'(V^\varepsilon) + 2U^\varepsilon\chi_0''(V^\varepsilon)V_z^\varepsilon\}\frac{d}{dz} + \{U^\varepsilon\chi_0''(V^\varepsilon)V_z^\varepsilon\}_z],$$

$$M^\varepsilon \equiv \frac{d^2}{dz^2} + \varepsilon\theta(\varepsilon)\frac{d}{dz} - \gamma.$$

For the eigenvalues of (3.2), we obtain the following lemmas:

LEMMA 2 *There is a constant $C_1 > 0$ and for any given $d > 0$ there is $\varepsilon_1 > 0$ such that any eigenvalue $\lambda \in \mathbf{C}$ of (3.2) satisfies either $Re\lambda < -C_1$ or*

$$|\varepsilon^2\omega^2 + \lambda| < d \quad \textit{for} \quad 0 < \varepsilon < \varepsilon_1 \quad \textit{and} \quad \omega > 0. \tag{3.3}$$

This lemma indicates that the distribution of eigenvalues of (3.2) is divided into two classes as $\varepsilon \downarrow 0$, that is, one class is the distribution of eigenvalues of the order $O(1)$ which have negative real part and the other is of the order $o(1)$. Therefore, one knows that the distribution of the latter eigenvalues is critical for the stability of travelling front solutions. By (3.3), we may assume that there is a positive function $d(\varepsilon)$ with $\lim_{\varepsilon\downarrow 0} d(\varepsilon) = 0$ such that

$$|\varepsilon^2\omega^2 + \lambda| < d(\varepsilon). \tag{3.4}$$

For eigenvalues of (3.2) satisfying (3.4), we have the following key lemma:

LEMMA 3. *For sufficiently small $\varepsilon > 0$, let λ_m be an eigenvalue of (3.2) which satisfies (3.4). Then, there exists a continuous function $\tau_m(\varepsilon, \ell, k)$ such that $\lambda_m = \varepsilon\tau_m(\varepsilon, \ell, k)$ satisfying*

$$\lim_{\varepsilon\downarrow 0}\{\tau_m(\varepsilon, \ell, k) - \tau_m^*(\varepsilon, \ell, k)\} = 0$$

with

$$\tau_m^*(\varepsilon, \ell, k) \equiv -\varepsilon(\frac{m\pi}{\ell})^2 + \frac{k}{4\sqrt{\gamma}}(\frac{1}{\sqrt{\gamma}} - \frac{1}{\sqrt{\gamma + (m\pi/\ell)^2}})\chi_0''(\frac{1}{2\gamma}). \tag{3.5}$$

When $m = 0$, we know $\tau_0^*(\varepsilon, \ell, k) = 0$, which corresponds to the zero eigenvalue of (3.2) with the eigenfunction $(U_z^\varepsilon, V_z^\varepsilon)(z)$ where $(U^\varepsilon, V^\varepsilon)(z)$ is the travelling front solution of (1.2). Lemmas 2 and 3 are proved in the next section. By using these lemmas with (3.5), we can easily arrive at the following theorem:

THEOREM 2.

(i) *When* $\chi_0''(\frac{1}{2\gamma}) \le 0$, *for any fixed* $\ell > 0$ *and* $k > 0$, *there is* $\varepsilon_0 > 0$ *such that if* $0 < \varepsilon < \varepsilon_0$, $\lambda_m < 0$ *holds for any* $m > 0$, *i. e. the travelling front solution is stable*;

(ii) *When* $\chi_0''(\frac{1}{2\gamma}) > 0$, *for any fixed* $\ell > 0$ *and* $k > 0$, *there is* $\varepsilon_0(\ell, k) > 0$ *such that for any* $0 < \varepsilon < \varepsilon_0(\ell, k)$, *the travelling front solution is unstable.*

It follows from Theorem 2 and (2.13) that transversal stability of travelling front solutions depends on the sign of $\chi_0''(v_{\rm I})$ where $v_{\rm I}$ is the value of v on the interface. In fact, when $\chi_0''(v_{\rm I}) > 0$, the travelling front solution is destabilized as k increases. Let ℓ be any fixed and $\lambda_{m_0(\varepsilon)}$ be the largest eigenvalue. Then, it follows from (3.5) that for sufficiently small ε, $m_0(\varepsilon)$ satisfies

$$\left| \varepsilon^{\frac{1}{3}} m_0(\varepsilon) - \frac{\ell}{2\pi} \left(\frac{k\chi_0''(\frac{1}{2\gamma})}{\sqrt{\gamma}} \right)^{\frac{1}{3}} \right| < \delta(\varepsilon),$$

where $\delta(\varepsilon)$ is a positive function satisfying $\lim_{\varepsilon \downarrow 0} \delta(\varepsilon) = 0$. Therefore, it turns out that the fastest growth wavelength $\mu_0(\varepsilon) = 2\ell/m_0(\varepsilon)$ satisfies $\mu_0(\varepsilon) = O(\varepsilon^{\frac{1}{3}})$ for sufficiently small ε. This implies that the wavelength $\mu_0(\varepsilon)$ does not depend on the width ℓ but on the smallness of ε, that is, when ε is sufficiently small, the destabilzed pattern initially exhibits any fine structure with $O(\varepsilon^{\frac{1}{3}})$.

Let us apply this theorem to two specific forms of $\chi_0(v)$. First, we take a simplest form $\chi_0(v) = v$. Since $\chi_0''(v) \equiv 0$, the travelling front solution is always transversally stable for any $k > 0$. We next take $\chi_0(v) = 8\sqrt{3s}v^2/9(s + v^2)$, for which there is some value $s^* = 3/4\gamma^2$ such that $\chi_0''(\frac{1}{2\gamma}) \le 0$ for $0 < s \le s^*$ and $\chi_0''(\frac{1}{2\gamma}) > 0$ for $s^* < s$. For the latter case, the bifurcation curves of $\tau_m^*(\varepsilon, \ell, k) = 0$ $(m = 1, 2, \cdots)$ are drawn in the (k, ℓ)-plane, as in Figure 3. This indicates the following:

(i) Let $k = k_m(\varepsilon, \ell)$ be a solution of $\tau_m^*(\varepsilon, \ell, k) = 0$ $(m = 1, 2, \cdots)$. Then it holds that $k_1(\varepsilon, \ell) < k_2(\varepsilon, \ell) < \cdots$ for any fixed $\ell > 0$.

(ii) There is the critical value $k_*(\varepsilon, \ell) = 4\varepsilon\gamma\sqrt{\gamma + (\pi/\ell)^2}(\sqrt{\gamma} + \sqrt{\gamma + (\pi/\ell)^2})\ /\chi_0''(\frac{1}{2\gamma})$ such that when $k < k_*(\varepsilon, \ell)$, $\lambda_m < 0$ holds for any $m > 0$, while when $k_*(\varepsilon, \ell) < k$, $\lambda_m > 0$ for some $m > 0$.

Figure 3 shows that for any fixed width $\ell > 0$, the travelling front solution is transversally destabilized as k increases. Let us show some numerical simulations for the problem (1.2), (1.8), (1.9) with $\chi_0(v) = 8v^2/3(3 + v^2)$ in Ω_ℓ with suitably large $\ell > 0$. When k is small, the travelling front solution is transversally stable. When k increases to satisfying $k > k_1(\varepsilon, \ell)$, it becomes unstable (Figure 4a). When k increases further, the travelling front solution evolves into a complex pattern (Figure 4b), where two features can be observed in the dynamics of patterns; one is tip–splitting to generate a branching pattern and the

other is coalescing of these branches, by which network–like structures appear. When k still increases further, the situation is drastically changed. The destabilized travelling front solution exhibits fingering–like pattern (Figure 4c). As was noted before, the interfaces are initially destabilized with small wavelengths of the order $O(\varepsilon^{\frac{1}{3}})$, but in the next stage, this fine structure breaks and there appear fingering–like branches with the width of the order $O(1)$.

4 Concluding Remarks

The numerical simulations suggest that chemotaxis has two effects; one is suppression of expanding patterns; the other is destabilization of disk–like patterns. For understanding these properties, we have studied the existence and transversal stability of 1–dimensional travelling front solutions in the strip domain. As was shown in Figure 2, that the velocity of travelling front solutions is positive for small k, while it is negative for large k. This clearly explains that the chemotactic effect inhibits the expansion of patterns. We have shown in Theorem 2 that transveral stability of travelling front solutions depends on the sign of $\chi_0''(1/2\gamma)$ of the chemotactic sensitivity function χ_0. When we specify $\chi_0(v) = 8v^2/3(3+v^2)$, it finds that $\chi_0''(1/2) = 2304/2197 > 0$ with $\gamma = 1$, that is, χ_0 satisfies the condition (ii) of Theorem 2 in this case. If k is small, the travelling front solution is transversally stable. However, when k increases, it becomes unstable through static bifurcation. If k increases further, the destabilized pattern exhibits tip–splitting and coalescing phenomena alternatively so that network–like pattern appears, as in Figure 4b. If k still increases, the pattern shrinks and generates finger–branched structures as in Figure 4c. This corresponds to finger–branched pattern obtained in Figure 1b. We should note that each branch grows as if it were a 2–dimensional travelling finger–like solution with constant velocity. In fact, the existence of 2–dimensional travelling finger solutions are numerically confirmed. When k is suitably large, we demonstrate in Figure 5 that the velocity of 1–dimensional travelling front solutions is negative, while the velocity of 2–dimensional travelling finger–like solutions is positive. For the possibility of existence of such 2–dimensional finger–like solutions, there are three plausible reasons by using the results obtained in [13]. (i) The travelling finger–like solution in $\mathbf{R}^2$ is regarded as a heteroclinic orbit connecting two stable states; one is $(0,0)$ at $y = \infty$ and the other is $(U_p(x), V_p(x))$ at $y = -\infty$ where $(U_p(x), V_p(x))$ is the 1–dimensional stable equilibrium pulse solution. (ii) The equilibrium pulse solution is transversally stable in the strip domain. This suggests that the side parts of a finger stably exists. (iii) 2–dimensional disk–like equilibrium solutions are unstable under 2–mode disturbance. As in Figure 6, a disk–like equilibrium solution destabilizes to form a peanut shape. It seems that this is the onset of travelling finger–like solutions. The rigorous

treatment of this solution will be a feature work.

References

1. Aronson, D. G. and Weinberger, H. F.: Nonlinear diffusion in population genetics, combustion and nerve propagation. In: Goldstein, J. A. (eds.) Partial Differential Equation and Related Topics. (Lect. Notes in Math. vol. 446) New York: Springer-Verlag, 5–49 1975
2. Aronson, D. G. and Weinberger, H. F.: Multidimensional nonlinear diffusion arising in population genetics. Advances in Mathematics **30**, 33–76 (1987)
3. Budrene, E. O. and Berg, H. C.: Complex patterns formed by motile cells of Escherichia coli. Nature **349**, 630–633 (1991)
4. Budrene, E. O. and Berg, H. C.: Dynamics of formation of symmetrical patterns by chemotactic bacteria. Nature **376**, 49–53 (1995)
5. Ezoe, H., Iwasa, Y. and Umeda, T.: Aggregation by chemotactic random walk: Drifting clusters and chemotactic friction. J. theor. Biol. **168**, 256–267 (1994)
6. Fife, P. C.: Boundary and interior transition layer phenomena for pairs of second–order differential equations. J. Math. Anal. Appl. **54**, 497–521 (1976)
7. Fife, P. C. and McLeod, J. B.: The approach of solutions of nonlinear diffusion equation to travelling wave solutions. Arch. Rational Mech. Anal. **65**, 335–361 (1977)
8. Ford, R. M. and Lauffenburger, D. A.: Analysis of chemotactic bacterial distributions in population migration essays using a mathematical model applicable to steep or shallow attractant gradients. Bull. Math. Biol. **53**, 721–749 (1991)
9. Jones, C. K. R. T. (1983) Spherically symmetric solutions of a reaction-diffusion equation, J. Differential Equations **49**, 142–169 (1983)
10. Jones, C. K. R. T.: Asymptotic behavior of a reaction-diffusion equation in higher space dimensions. Rocky Mountain J. Math. **13**, 355–364 (1983)
11. Kawasaki, K. and Shigesada, N.: Modeling pattern formation of chemotactic bacteria. manuscript
12. Mimura, M., Tabata, M. and Hosono, Y.: Multiple solutions of two–point boundary value problems of Neumann type with a small parameter. SIAM J. Math. Anal. **11**, 613–631 (1980)
13. Mimura, M. and Tsujikawa, T.: Aggregating pattern dynamics in a chemotaxis model including growth. Physica A **230**, 499–543 (1996)
14. de Mottoni, P. and Schatzman, M.:Geometrical evolution of developed interfaces. Trans. AMS **347**, 1533–1589 (1995)
15. Murray, J. D.: Mathematical Biology. Springer-Verlag, Berlin (1989)
16. Nishiura, Y. and Fujii, H.: Stability of singularly perturbed solutions to systems of reaction–diffusion equations. SIAM J. Math. Anal. **18**, 1726–1770 (1987)
17. Schaaf, R.: Stationary solutions of chemotaxis system. Trans. AMS **292**, 531–556

(1985)
18. Stevens, A.: Trail following and aggregation of myxobacteria. Biol. Systems **3**, 1059–1068 (1995)
19. Taniguchi, M.: Instability of planar traveling fronts in bistable reaction-diffusion systems. submitted
20. Tsimring L. and Levine H.: Aggregation patterns in stressed bacteria. Phys. Rev. Lett. **75**, 1859–1862 (1995)
21. Tsujikawa, T.: Singular limit analysis of planar equilibrium solutions to a chemotaxis model equation with growth. Methods Appl. Anal. **3**, 401–431 (1996)
22. Volpert, A., Volpert, Vit. A. and Volpert, Vl. A.: Traveling wave solutions of parabolic system. AMS, Providence, Rhode Island 1994
23. Woodward, D. E., Tyson, R., Myerscough, M., R., Murray, J. D., Budrene, E. O. and Berg, H. C.: Spatio-temporal patterns generated Salmonella typhimurium. Biophys. **68**, 2181–2189 (1995)

Captions

Figure 1: Time evolution of $u(t, \mathbf{x})$ under non–radially symmetric initial conditions, where the curve means the contour $C(t) = \{\mathbf{x} \in \mathbf{R}^2 | u(t, \mathbf{x}) = 0.1\}$. Parameters are choosen as $\varepsilon = 0.05$, $a = 0.1$ and $\gamma = 1.0$ and the system size is 20×20. (a) Formation of network–like pattern ($k = 2.0$). (b) Formation of finger–like pattern ($k = 5.0$).

Figure 2: Dependency of the velocity $\theta^*(k)$ on k of travelling front solution where $\square$ means the numerical velocity solved by (2.6). The parameters except for k are the same as the ones in Figure 1.

Figure 3: Bifurcation curves $k = k_m(\varepsilon, \ell)$ $(m = 1, 2, \cdots)$ of the flat travelling front solution where $\chi_0(v) = 8v^2/3(3 + v^2)$. The parameters except for k are the same as the ones in Figure 1. Here m is the mode number of perturbations and $k_1^*(\varepsilon) = \lim_{\ell \to \infty} k_1(\varepsilon, \ell)$.

Figure 4: Time evolution of $u(t, \mathbf{x})$, where the curves depict the contour $C(t) = \{\mathbf{x} \in \Omega_\ell | u(t, \mathbf{x}) = 0.1\}$, where the parameters are the same as the ones in Figure 1 except the system size 10×30. (a) Destabilized travelling front solution ($k = 1.0$). (b) Formation of the network–like pattern ($k = 2.0$). (c) Formation of the finger–like pattern ($k = 5.0$).

Figure 5: $\diamondsuit$ means the velocity of 2–dimensional travelling finger–like solutions, where the parameters are the same as the ones in Figure 1. —— means the velocity $\theta^*(k)$ of 1–dimensional travelling front solutions as $\varepsilon \downarrow 0$.

Figure 6: Time evolution of $u(t, \mathbf{x})$ under non–radially symmetric initial conditions, where the curve means the contour $C(t) = \{\mathbf{x} \in \mathbf{R}^2 | u(t, \mathbf{x}) = 0.1\}$. Parameters are the same as the ones in Figure 1 except $k = 5.0$ and the system size 20×20.

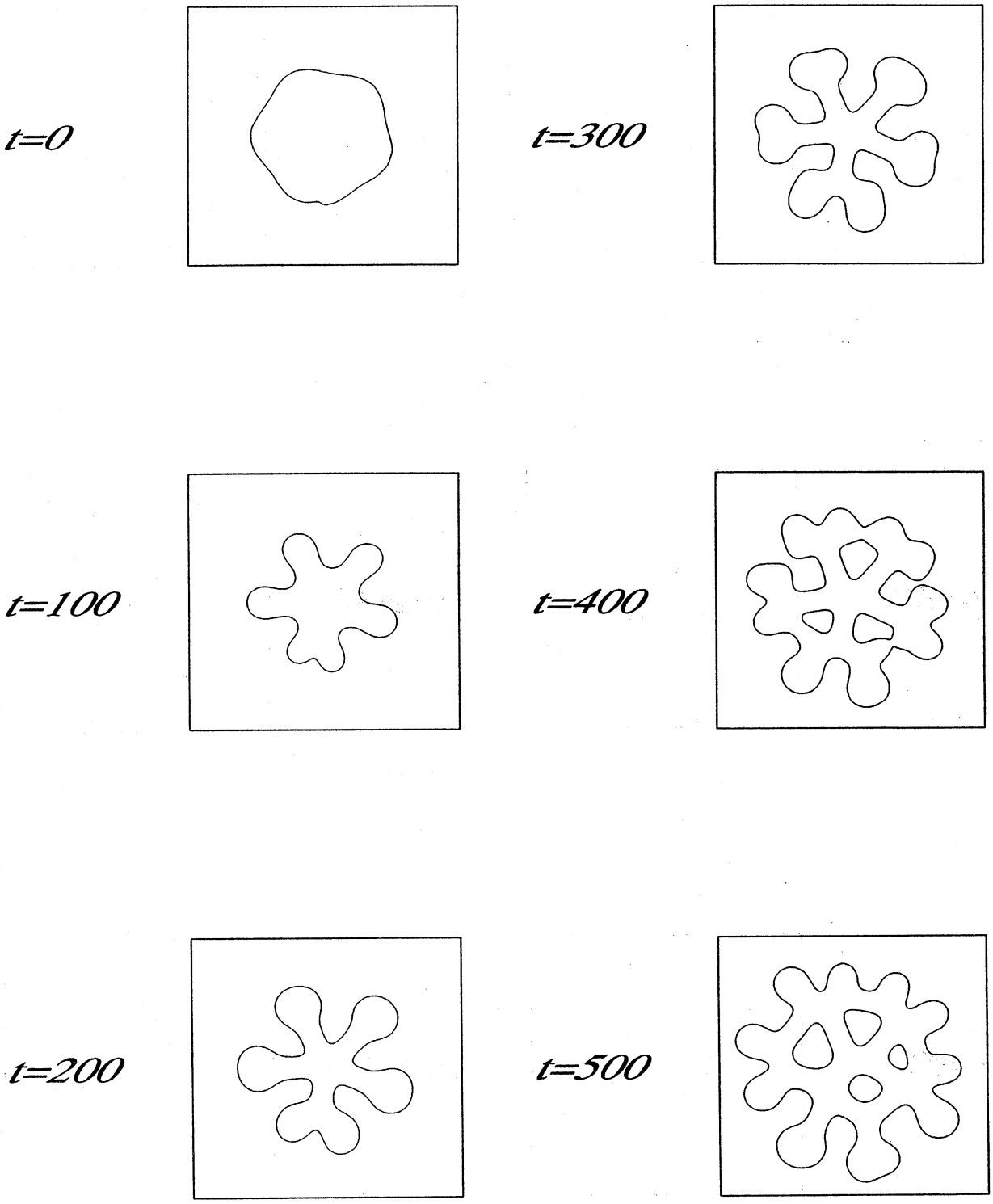

Figure 1a

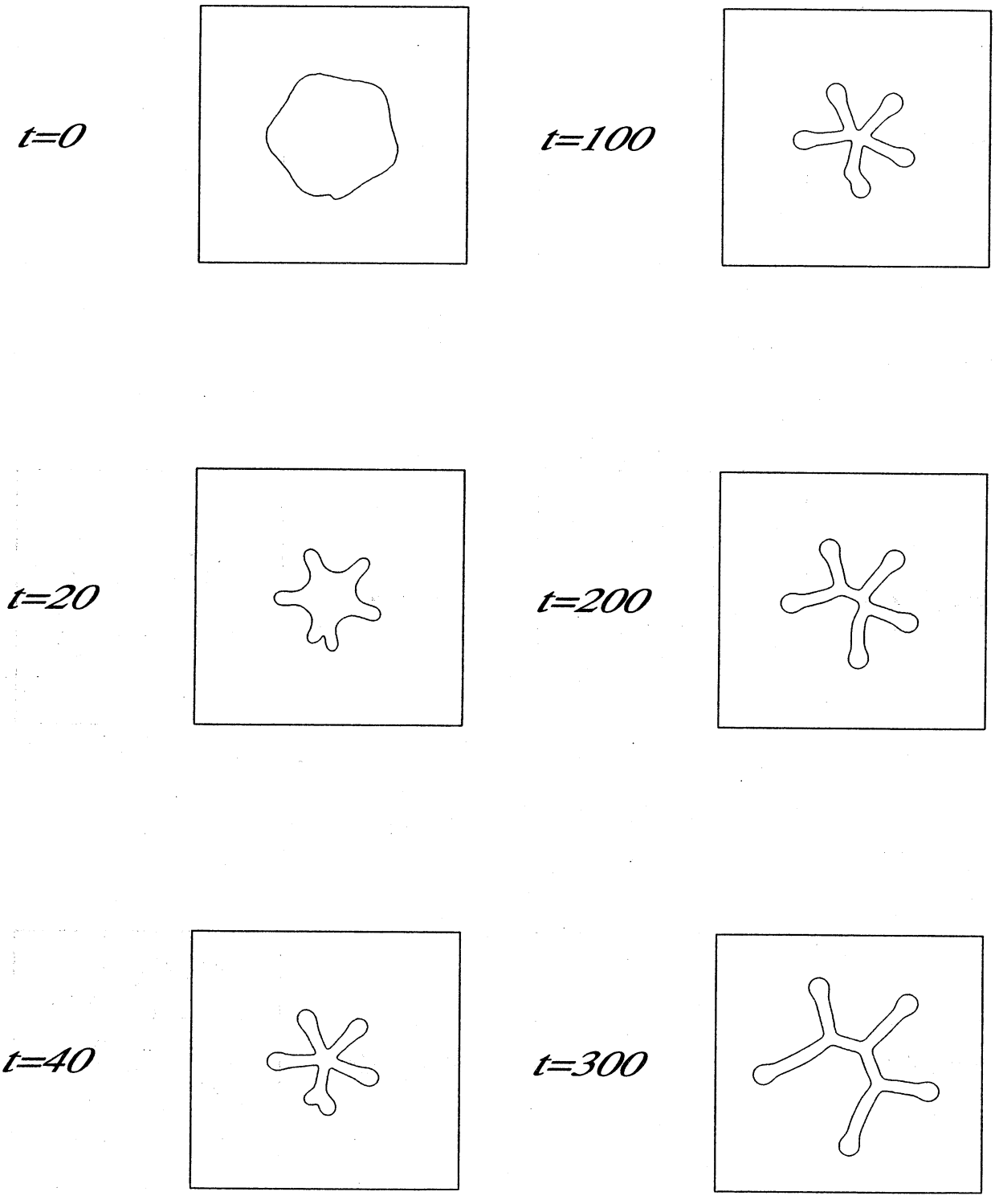

Figure 1b

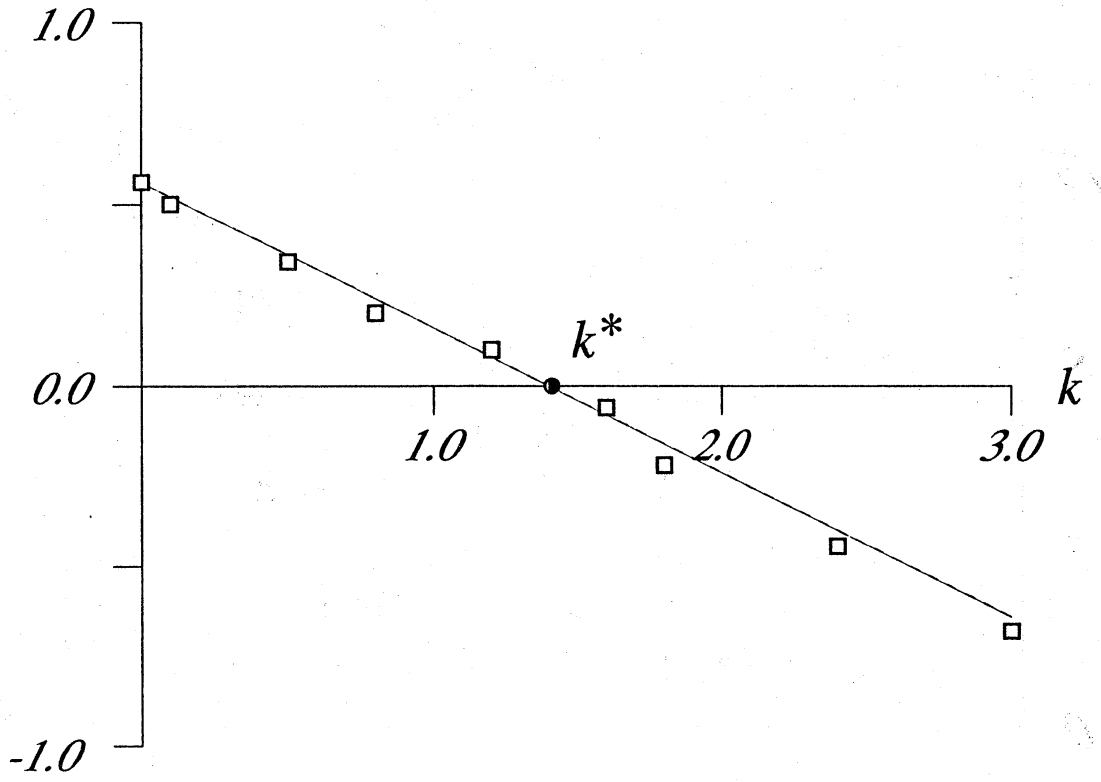

Figure 2

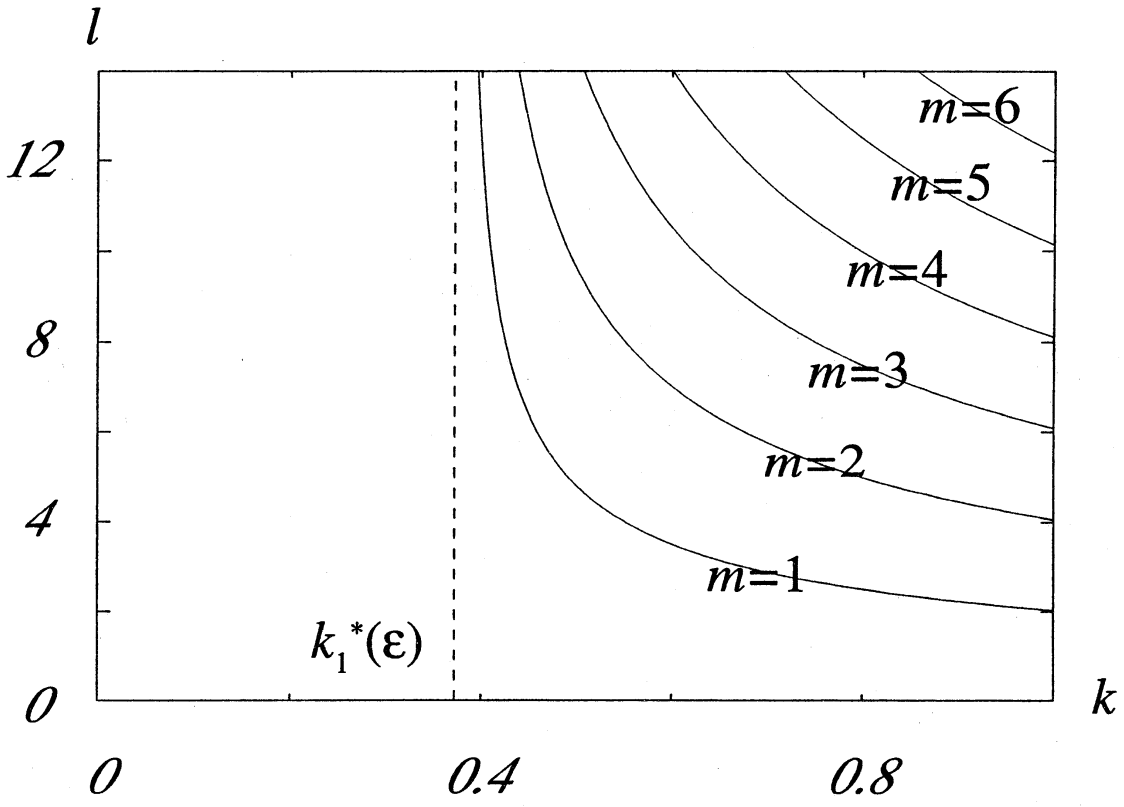

Figure 3

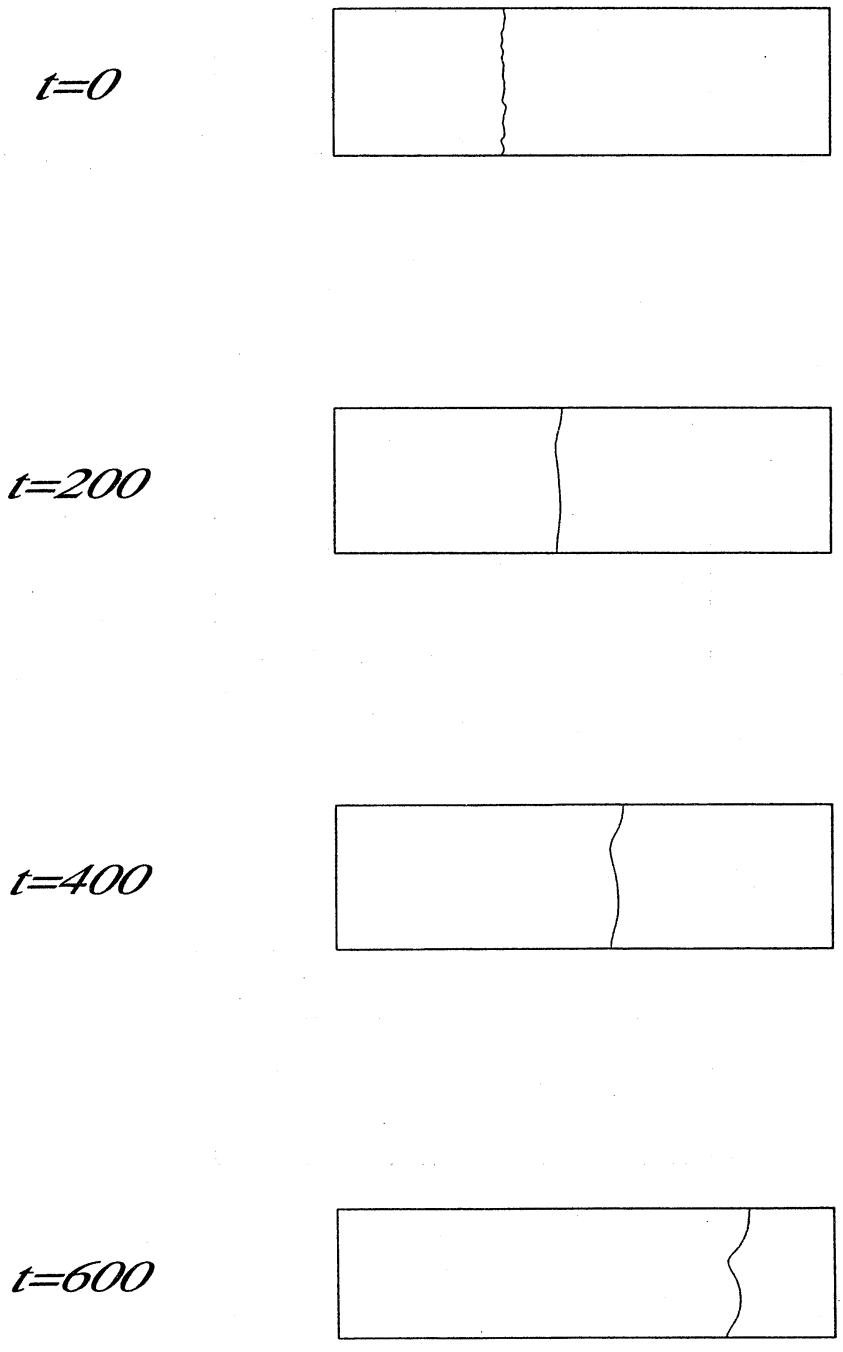

Figure 4a

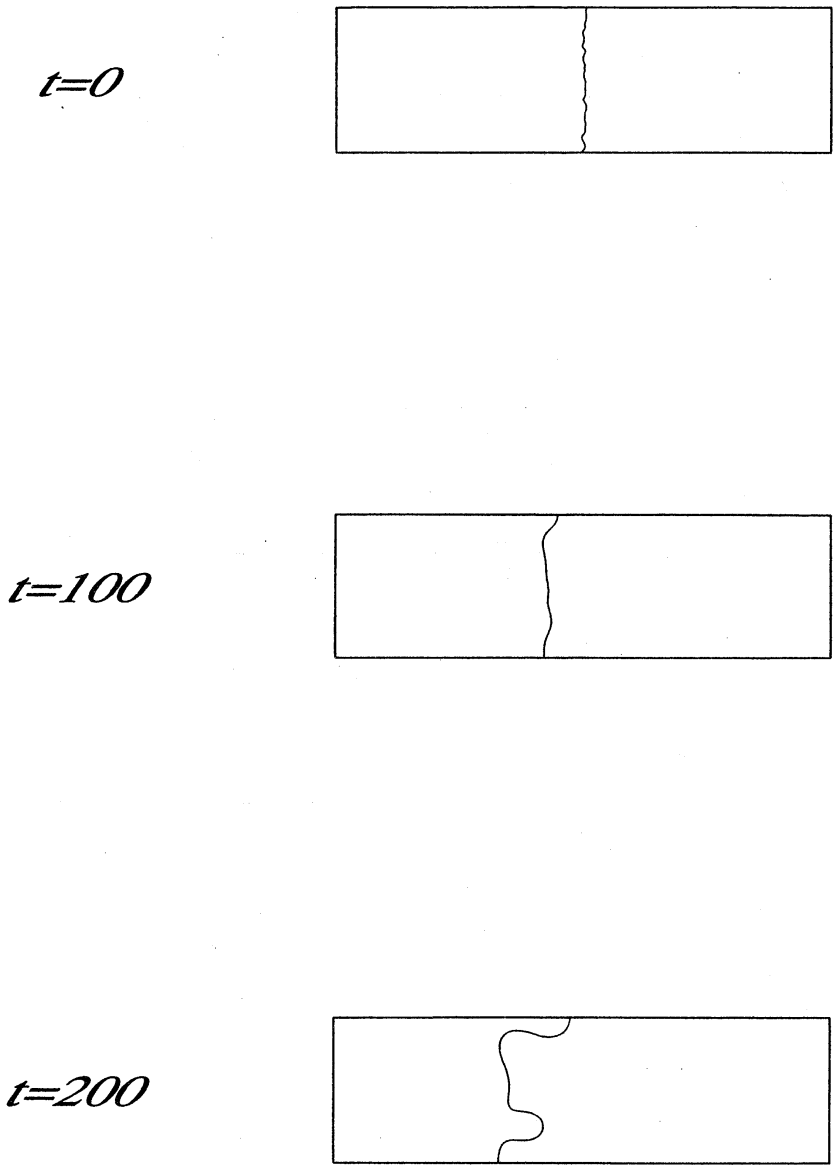

Figure 4b1

t=300

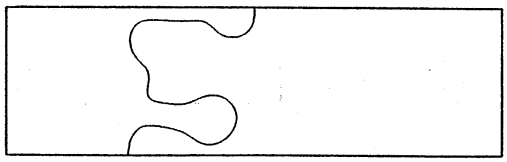

t=400

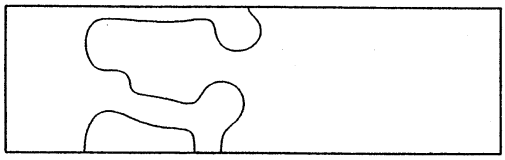

t=500

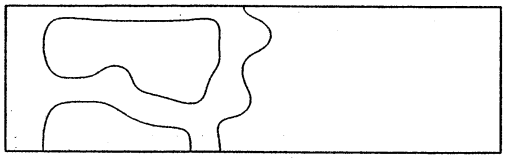

Figure 4b2

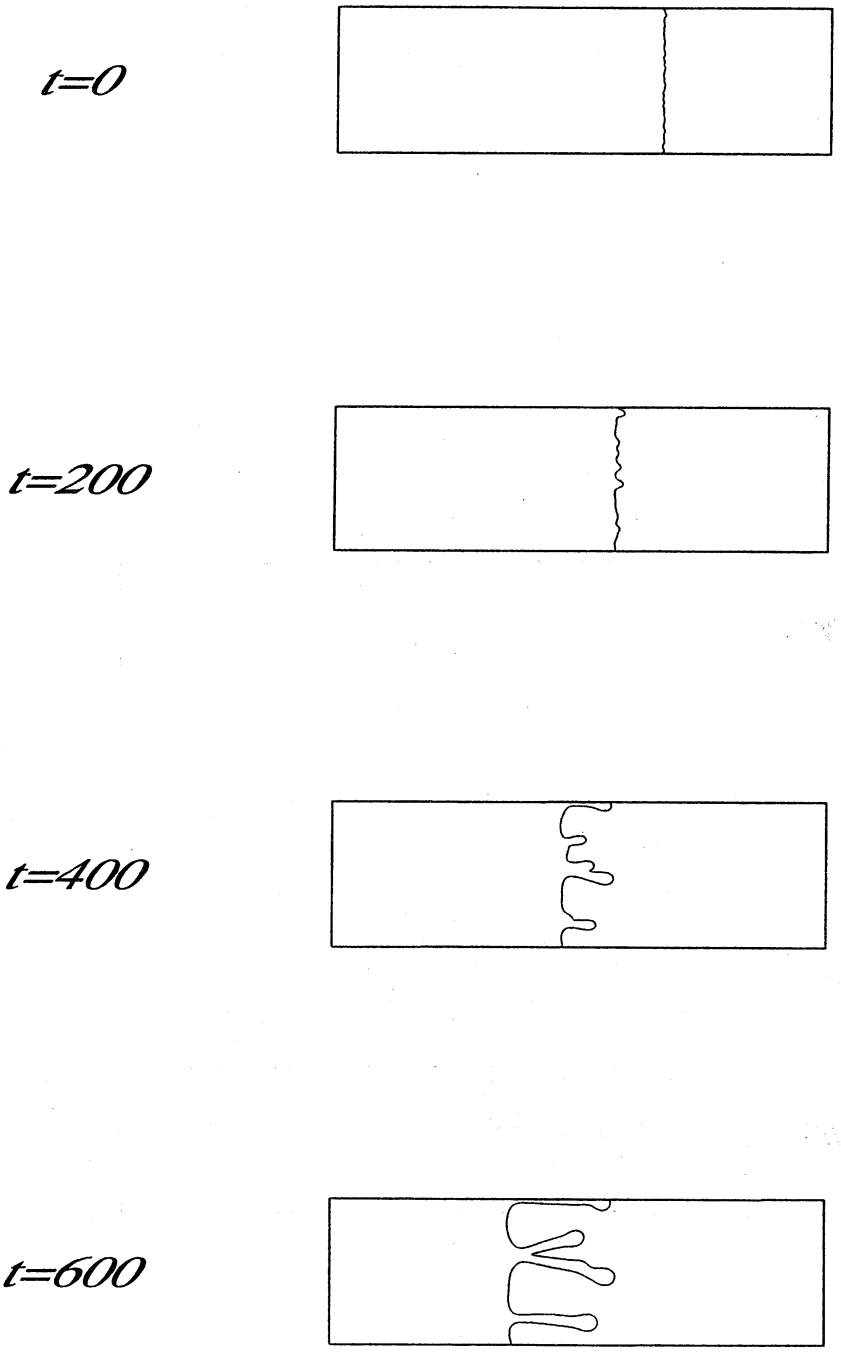

Figure 4c

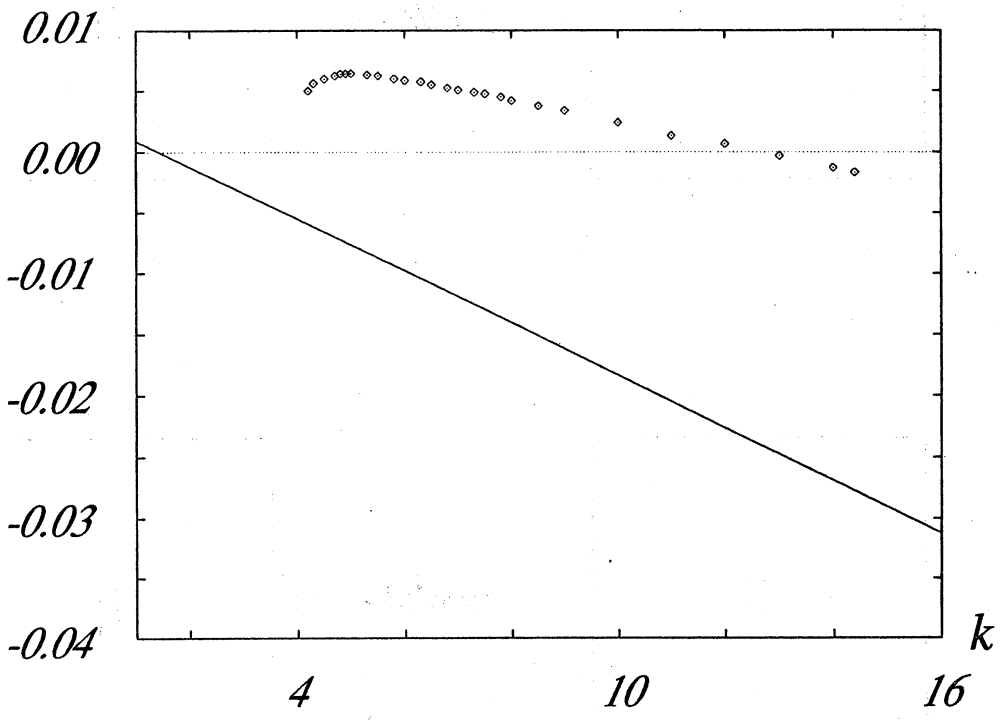

Figure 5

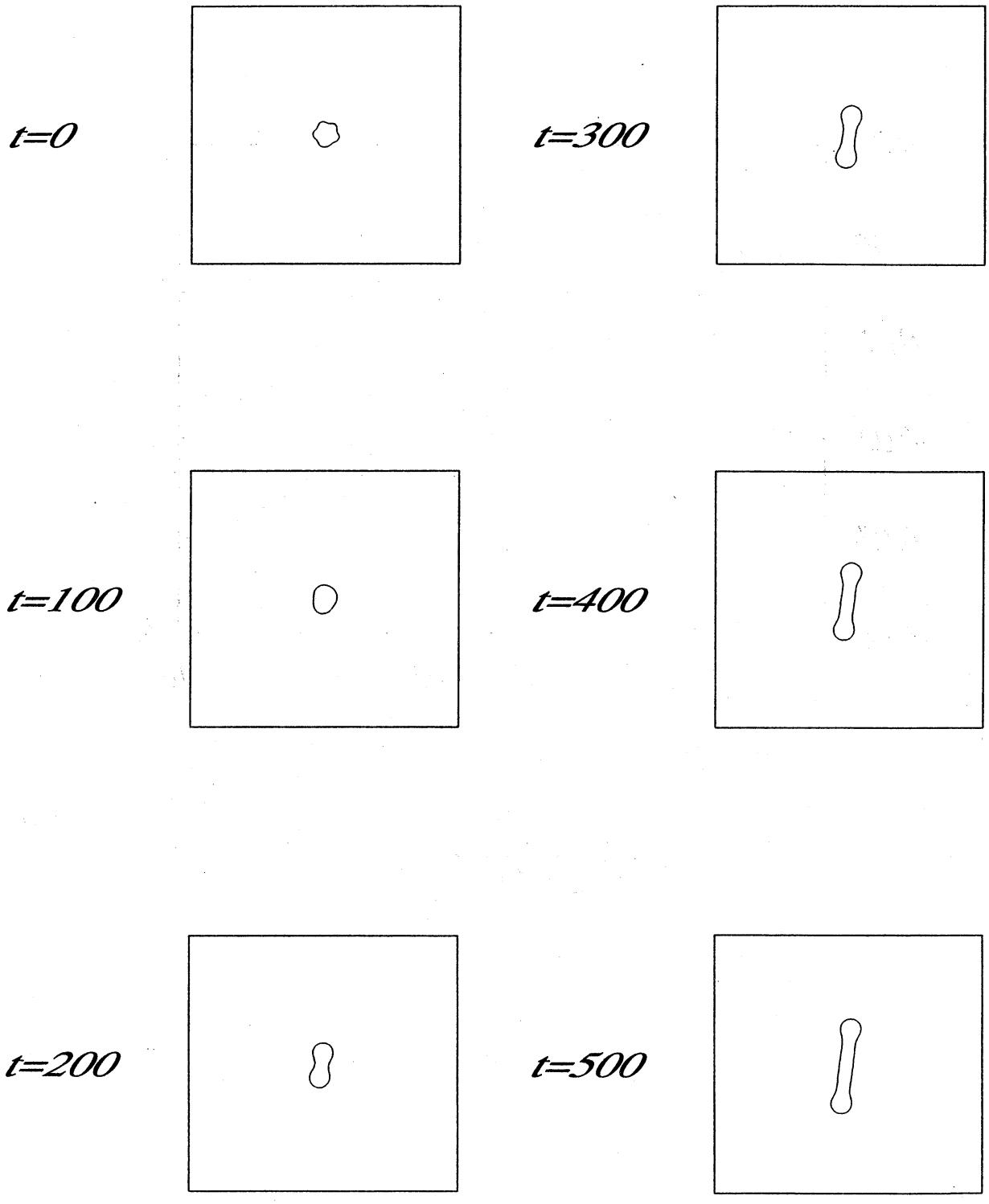

Figure 6